Hard parton dispersion in the quark-gluon plasma, non-perturbatively

Jacopo Ghiglieri,[a,*] **Guy D. Moore,**[b] **Philipp Schicho,**[c] **Niels Schlusser**[d] **and Eamonn Weitz**[a]

[a] *SUBATECH, Nantes Université, IMT Atlantique, IN2P3/CNRS,*
  4 rue Alfred Kastler, La Chantrerie BP 20722, 44307 Nantes, France

[b] *Institut für Kernphysik, Technische Universität Darmstadt,*
  Schlossgartenstrasse 2, D-64289 Darmstadt, Germany

[c] *Institute for Theoretical Physics, Goethe Universität Frankfurt, 60438 Frankfurt, Germany*

[d] *Biozentrum, University of Basel, Spitalstrasse 41, 4056 Basel, Switzerland*
  E-mail: jacopo.ghiglieri@subatech.in2p3.fr,
  guy.moore@physik.tu-darmstadt.de, schicho@itp.uni-frankfurt.de,
  niels.schlusser@unibas.ch, eamonn.weitz@subatech.in2p3.fr

The in-medium dispersion of hard partons, encoded in their so-called asymptotic mass, receives large non-perturbative contributions from classical gluons, i.e. soft gluons with large occupation numbers. Here, we discuss how the analytical properties of thermal amplitudes allow for a non-perturbative determination of the infrared classical contribution through lattice determinations in the dimensionally-reduced effective theory of hot QCD, EQCD. We show how these lattice determinations need to be complemented by perturbative two-loop matching calculations between EQCD and QCD, so that the unphysical (classical) ultraviolet behavior of EQCD is replaced by its proper quantum QCD counterpart. We show how lattice and perturbative EQCD are in good agreement in the UV and present an outlook on the two-loop quantum QCD contribution.

---

*Speaker

1. Introduction

Jets are a key *hard probe* in the theoretical and experimental investigation of the Quark-Gluon Plasma (QGP), an exotic state of strongly interacting matter. Their study provides important experimental sources of evidence about the nature of Quantum Chromodynamics (QCD) under extreme conditions – see [1–3] for recent reviews.

Here, we focus on jets created by light quarks (u, d, s) or gluons. While massless in vacuum, high-energy particles with momentum $\boldsymbol{p}$ follow the dispersion relation of massive particles when traversing a QGP of temperature T, $\omega_{\boldsymbol{p}}^2 = \boldsymbol{p}^2 + m_{\boldsymbol{p}}^2$, as found independently by Klimov [4] and Weldon [5, 6]. This effective mass arises through *forward scattering* with the medium. At very large momentum, it is called the *asymptotic mass* and it is an important ingredient in the determination of medium-induced radiation rates and transport coefficients, see [7] for a review.

To one-loop order, these masses are given by the gauge and the fermion condensates Z_g and Z_f:

$$m_{\infty,q}^2 = g^2 C_F \left(Z_g + Z_f \right), \qquad m_{\infty,g}^2 = g^2 C_A Z_g + 2g^2 T_F N_f Z_f, \qquad (1)$$

where $m_{\infty,q}^2$ for quarks and $m_{\infty,g}^2$ for gluons. Here $C_F = 4/3$ and $C_A = 3$ are the quark and gluon quadratic Casimir, N_f is the number of light quark species, and $T_F = 1/2$ is the trace normalization of the fundamental representation. The condensates Z_g and Z_f are non-local and have a gauge-invariant definition in terms of correlators [8, 9]

$$Z_f \equiv \frac{1}{6} \left\langle \overline{\psi} \frac{v_\mu \gamma^\mu}{v \cdot D} \psi \right\rangle, \qquad Z_g \equiv -\frac{1}{8} \left\langle v_\alpha F^{\alpha\mu} \frac{1}{(v \cdot D)^2} v_\nu F^\nu_{\ \mu} \right\rangle, \qquad (2)$$

where $v^\mu = (1, 0, 0, 1)$ is the four-velocity of the hard particle and $\langle \ldots \rangle$ denotes a thermal expectation value. Our conventions are as in [10].

Eq. (1) arises from integrating out the energy scale of the jet $p \sim E \gg T$, truncating at first order in T/E and determining the matching coefficients at $O(g^0)$. If $E \gtrsim T$, higher orders in the T/E expansion can become relevant beyond one-loop order and spoil the factorization into fermionic and bosonic condensates of (1). In coordinate space, the inverse of a covariant derivative is an integral over separation of a Wilson line U. Z_g is then an integral over $x^+ \equiv (x^0 + x^z)/2$ of a correlator of two Lorentz-force insertions

$$Z_g \equiv -\frac{1}{4} \int_0^\infty dx^+ x^+ \, \text{Tr} \left\langle U(-\infty; x^+) v_\mu F^{\mu\nu}(x^+) \, U(x^+; 0) \, v_\rho F^\rho_{\ \nu}(0) U(0; -\infty) \right\rangle, \qquad (3)$$

with $F_{\mu\nu} = F_{\mu\nu}^a T^a$. T^a is in the fundamental representation. So are the Wilson lines, which source path-ordered gluons along the x^+ light-cone direction. At leading order (LO), one easily finds [4–6]

$$Z_g\big|^{LO} = \frac{1}{\pi^2} \int_0^\infty dq \, q \, n_B(q) = \frac{T^2}{6}, \qquad Z_f\big|^{LO} = \frac{1}{\pi^2} \int_0^\infty dq \, q \, n_F(q) = \frac{T^2}{12}. \qquad (4)$$

The first correction to this affects Z_g only and does not come from extra loops but from a more careful evaluation of the infrared (IR). As $n_B(q \ll T) \approx \frac{T}{q} \gg 1$, soft ($q \sim gT$) gluons are *classical* and their contribution represents an $O(g)$ correction, which can be evaluated by properly accounting for the collective effects that arise at that scale. This was done in [9], yielding the next-to-leading order (NLO) *viz.* $Z_g\big|^{NLO} = -Tm_D/(2\pi)$, where $m_D = gT\sqrt{1 + N_f/6}$ is the Debye mass. This remarkable

result was obtained, following [11], by exploiting the analytical properties of thermal amplitudes at space- and light-like separations to map the classical contribution to Eq. (3) to its counterpart Z_g^{3d} in Electrostatic QCD (EQCD). EQCD [12–16] is a dimensionally-reduced (3D) Effective Field Theory (EFT) that describes the Matsubara zero-modes of the gauge fields, integrating out all non-zero quark and gluon modes.

This mapping is remarkable: as Z_g^{3d} can be determined non-perturbatively in lattice EQCD, this then gives an all-order determination of the classical contribution to Z_g. In general, the classical soft and ultrasoft ($q \sim g^2 T$) modes are responsible for the slow convergence — or outright breakdown in the latter case [17] — of thermal perturbation theory. Hence, the availability of a non-perturbative determination circumvents this issue. In this contribution, we then discuss the necessary steps in lattice and continuum EQCD, as well as in perturbative thermal QCD, to reach this goal. This is based on [10, 18, 19], to which we refer for further details. A similar program has already been carried out in [20, 21] for the transverse scattering kernel.

2. Lattice determination

The continuum EQCD action reads

$$S_{\text{EQCD},c} = \int_{\mathbf{x}} \left\{ \frac{1}{2} \text{Tr} \, F_{ij} F_{ij} + \text{Tr} \, [D_i, \Phi][D_i, \Phi] + m_{\text{D}}^2 \text{Tr} \, \Phi^2 + \lambda_{\text{E}} (\text{Tr} \, \Phi^2)^2 \right\}. \tag{5}$$

Under dimensional reduction A^0 becomes an adjoint scalar, $A^0 \to -i\Phi$, $\lambda_{\text{E}} \sim g^4 T$ and $g_{3d}^2 \approx g^2 T$ is the dimensionful gauge coupling [16], making EQCD super-renormalizeable. The EQCD contribution to Eq. (3) is then

$$Z_g^{3d} = \frac{T}{2} \int_0^\infty \mathrm{d}L \, L \, \langle FF \rangle, \text{ where } \langle FF \rangle \equiv \left(\langle EE \rangle - \langle BB \rangle - i\langle EB \rangle \right), \text{ and } E = D_x \Phi, \; B = F_{xz}. \tag{6}$$

$\langle EE \rangle \equiv \frac{1}{2} \langle (D_x \Phi(L))^a \, \tilde{U}_{\text{A}}^{ab}(L,0) \, (D_x \Phi(0))^b \rangle$ and similarly for $\langle BB \rangle$ and $i\langle EB \rangle$. Under dimensional reduction $x^+ \to L$, which, together with the rotation of A^0 in the complex plane, turns the adjoint Wilson line into a non-unitary 3D equivalent $\tilde{U}_{\text{A}}^{ab}(L,0)$, see [18].

Lattice EQCD provides us with continuum-extrapolated values for the three correlators $\langle EE \rangle$, $\langle BB \rangle$ and $i\langle EB \rangle$ at discrete values of the separation L in the range $0.25 < g_{3d}^2 L < 3$ at four different temperatures — see [10, 18] for details on discretization, renormalization and continuum extrapolation. Eq. (6) requires an integral over all values of L. The IR range at large $g_{3d}^2 L \gg 1$ can be addressed by a fitting ansatz based on the expected exponential falloff from electrostatic and magnetostatic screening. At short distances, on the other hand, not only are we limited by lattice spacing and increasing discretization effects, but we need to address the fact that the UV of EQCD, as for any IR EFT, differs from the UV of QCD, as we now discuss.

3. Ultraviolet matching

In the deep UV ($m_{\text{D}} L \ll 1$), we expect perturbative EQCD (pEQCD) to be applicable; furthermore, this is where super-renormalizability comes in handy, since it dictates that

$$\langle FF \rangle_{m_{\text{D}} L \ll 1} = \frac{c_0}{L^3} + \frac{c_2 g_{3d}^2}{L^2} + \frac{c_4 g_{3d}^4}{L} + \dots, \tag{7}$$
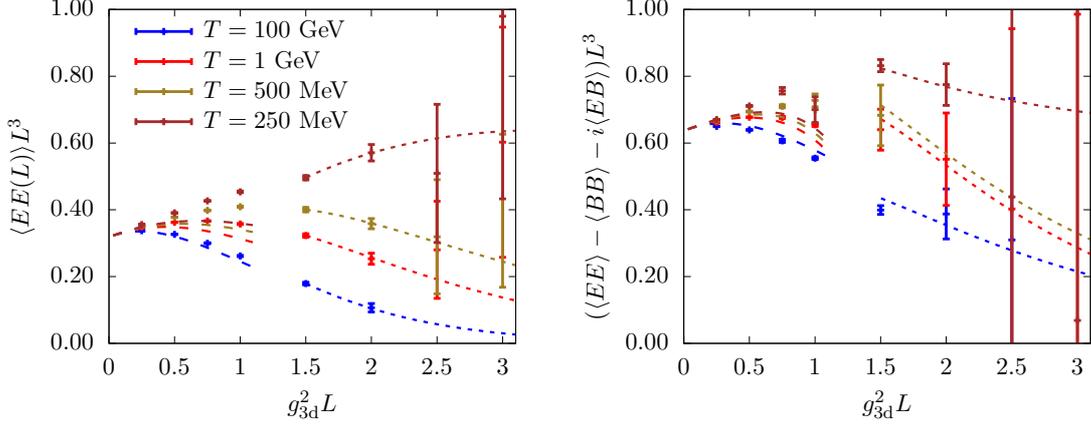
Figure 1: Continuum-extrapolated EQCD lattice data on $\langle EE \rangle$ and $\langle FF \rangle$ in eq. (6) with modelled long L-tail (short dashes) and NLO pEQCD (long dashes). L^3 compensates the c_0/L^3 divergence. Figure from [10].

with constants c_i arising from short-distance pEQCD. Only the first two terms will be divergent when plugged in Eq. (6). c_0/L^3 gives rise to a power-law divergence: indeed, the classical contribution to Eq. (4), obtained from $n_B(q) \to \frac{T}{q}$, is linearly UV divergent. These two divergences are opposite and, if evaluated in the same scheme, cancel: the UV of EQCD, where m_D and λ_E are negligible, must agree with the IR of bare 4D QCD. As the bare 4D QCD IR is included in Eq. (4), we can simply subtract c_0/L^3 $\forall L$ on the EQCD side. A simple calculation finds $c_0 = 2/\pi$.

At NLO in pEQCD, $c_2 g_{3d}^2/L^2$ gives rise to a logarithmic divergence, namely a $c_2 g_{3d}^2 T \ln(\mu/m_D)/2$ contribution to Z_g^{3d}, with μ a generic UV regulator. This must necessarily be complemented by a $c_2 g^2 T^2 \ln(T/\mu)/2$ contribution from bare 4D QCD at $O(g^2)$. The latter will be the focus of Sec. 4.

In [10] we then computed $\langle FF \rangle_{\text{NLO}}$, the NLO correction to Z_g^{3d} in pEQCD; expanded for $m_D L \ll 1$ this yields $c_2 = 3/(2\pi^2)$. In Fig. 1 we show our lattice data for the $\langle EE \rangle$ and $\langle FF \rangle$ channels compared with the pEQCD evaluation and IR ansatz. As one can see, pEQCD and lattice agree at the very least at the smallest separation. We can then merge the two as follows

$$Z_g^{3d}\Big|^{\text{merge}} = \frac{T}{2}\Bigg\{ \int_0^{L_{\min}} dL\, L\bigg[\langle FF \rangle_{\text{NLO}} - \frac{c_0}{L^3} - \frac{c_2 g_{3d}^2}{L^2} \bigg] + \int_{L_{\min}}^{L_{\max}} dL\, L\bigg[\langle FF \rangle_{\text{lat}} - \frac{c_0}{L^3} \bigg]$$
$$+ \int_{L_{\max}}^{\infty} dL\, L\bigg[\langle FF \rangle_{\text{tail}} - \frac{c_0}{L^3} \bigg] \Bigg\}, \tag{8}$$

where $L_{\min}$ and $L_{\max}$ are the smallest and largest separations on the lattice and $\langle FF \rangle_{\text{lat}}$ and $\langle FF \rangle_{\text{tail}}$ are the lattice and IR tail determinations. This procedure can be understood as splitting the integration into three regions: from left to right these are the pEQCD, lattice and IR tail ones. As the c_2-term is only subtracted in the perturbative region, Eq. (8) introduces an artificial logarithmic dependence on its boundary $L_{\min}$. Further details and numerical results for this procedure are available in [10].

4. Perturbative determination and outlook

To lift this artificial cutoff dependence on $L_{\min}$, in [19] we set out to determine the two-loop contribution to Z_g in thermal 4D QCD for loop four-momenta of order T. In principle this requires
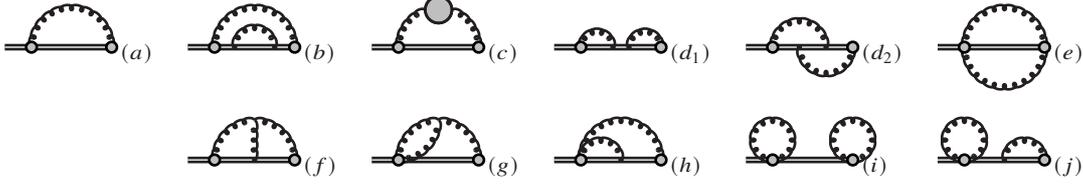
Figure 2: Diagrams contributing to Z_g at LO and NLO. Gray shaded vertices denote $F^{-\perp}$ insertions; a solid line a Wilson line; and a curly line a gluon, with the blob its self-energy. See [10] for the EQCD counterpart.

the evaluation of diagrams (b)–(j) in Fig. 2. Using the equation of motion of the Wilson line, we can show that only diagram (c) contributes in Feynman gauge.

There we identify the IR-divergent contribution as arising from a thermal momentum, $K \sim T$ in the blob and a soft one in the outer integration, $Q \sim gT$. We carefully evaluate it in dimensional regularization; we do the same for the $-c_2 g_{3d}^2 \theta(L_{\min} - L)/L^2$ subtraction in Eq. (8), finding that UV and IR poles cancel as expected, yielding this new matching term [19]

$$Z_g^{\text{match}} = \frac{3g^2 T^2}{4\pi^2}\left[\ln(2L_{\min}T) + \gamma_{\text{E}} - \frac{3}{2}\right], \qquad Z_g^{\text{non-pert class}} = Z_g^{3d}\Big|^{\text{merge}} + Z_g^{\text{match}} . \tag{9}$$

The $\ln(L_{\min})$ dependence vanishes in $Z_g^{\text{non-pert class}}$, the sum of Eq. (8) and Z_g^{match}. $Z_g^{\text{non-pert class}}$ thus provides the complete non-perturbative determination of the classical contribution to Z_g. Numerically, this combination results in a negative contribution to Z_g which is in magnitude larger than the negative $Z_g\big|^{\text{NLO}} = -T m_{\text{D}}/(2\pi)$. Physically, negativity can be understood as follows. Let us consider the soft sector of bare 4D QCD. At LO Eq. (4) implies $Z_g\big|_{\text{bare LO}}^{\text{soft}} = \frac{1}{\pi^2}\int_{gT} dq\, q\, T/q$. Our procedure amounts to subtracting this bare soft sector and replacing it with its screened EQCD counterpart, which reduces its contribution.

Before conclusions on the convergence of this EQCD approach can be drawn, it must be noted that Z_g^{match} only contains the part of the two-loop 4D QCD calculation responsible for the IR limit, and that this separation is to some degree arbitrary. Only the full determination of the two-loop 4D QCD contribution to Z_g will allow a definite conclusion.[1] Preliminary results [19] further indicate the likely emergence of *collinear modes* at this order in perturbation theory. These modes have energies of order E at small angles to $\boldsymbol{p}$, see [25] for the interplay of collinear and classical modes in transverse momentum broadening.

Acknowledgments

---

[1]This is a distinct problem from the one recently tackled in [22–24], namely the two-loop and power corrections to Hard Thermal Loops and their relation to the asymptotic mass for quasiparticles obeying $T \gg p \gg gT$.

References

[1] M. Connors, C. Nattrass, R. Reed and S. Salur, *Rev. Mod. Phys.* **90** (2018) 025005 [1705.01974].

[2] L. Cunqueiro and A.M. Sickles, *Prog. Part. Nucl. Phys.* **124** (2022) 103940 [2110.14490].

[3] L. Apolinário, Y.-J. Lee and M. Winn, *Prog. Part. Nucl. Phys.* **127** (2022) 103990 [2203.16352].

[4] V. Klimov, *Sov. Phys. JETP* **55** (1982) 199.

[5] H. Weldon, *Phys. Rev. D* **26** (1982) 1394.

[6] H. Weldon, *Phys. Rev. D* **26** (1982) 2789.

[7] J. Ghiglieri, A. Kurkela, M. Strickland and A. Vuorinen, *Phys. Rept.* **880** (2020) 1 [2002.10188].

[8] E. Braaten and R.D. Pisarski, *Phys. Rev. D* **45** (1992) 1827.

[9] S. Caron-Huot, *Phys. Rev. D* **79** (2009) 125002 [0808.0155].

[10] J. Ghiglieri, G.D. Moore, P. Schicho and N. Schlusser, *JHEP* **02** (2022) 058 [2112.01407].

[11] S. Caron-Huot, *Phys. Rev.* **D79** (2009) 065039 [0811.1603].

[12] E. Braaten, *Phys.Rev.Lett.* **74** (1995) 2164 [hep-ph/9409434].

[13] E. Braaten and A. Nieto, *Phys. Rev.* **D51** (1995) 6990 [hep-ph/9501375].

[14] E. Braaten and A. Nieto, *Phys.Rev.* **D53** (1996) 3421 [hep-ph/9510408].

[15] K. Kajantie, M. Laine, K. Rummukainen and M.E. Shaposhnikov, *Nucl.Phys.* **B458** (1996) 90 [hep-ph/9508379].

[16] K. Kajantie, M. Laine, K. Rummukainen and M.E. Shaposhnikov, *Nucl. Phys.* **B503** (1997) 357 [hep-ph/9704416].

[17] A.D. Linde, *Phys. Lett.* **96B** (1980) 289.

[18] G.D. Moore and N. Schlusser, *Phys. Rev. D* **102** (2020) 094512 [2009.06614].

[19] J. Ghiglieri, P. Schicho, N. Schlusser and E. Weitz, *in preparation* (2023) .

[20] G.D. Moore and N. Schlusser, *Phys. Rev. D* **101** (2020) 014505 [1911.13127].

[21] G.D. Moore, S. Schlichting, N. Schlusser and I. Soudi, *JHEP* **10** (2021) 059 [2105.01679].

[22] A. Ekstedt, *JHEP* **06** (2023) 135 [2302.04894].

[23] A. Ekstedt, 2304.09255.

[24] T. Gorda, R. Paatelainen, S. Säppi and K. Seppänen, 2304.09187.

[25] J. Ghiglieri and E. Weitz, *JHEP* **11** (2022) 068 [2207.08842].